

Arylmethoxyphenyl Derivatives: Small Molecules Displaying P-Glycoprotein Inhibition

Nicola Antonio Colabufo,*[‡] Francesco Berardi,[†] Roberto Perrone,[†] Simona Rapposelli,*[‡] Maria Digiacomo,[‡] and Aldo Balsamo[‡]

Dipartimento Farmacochimico, Università degli Studi di Bari, Via Orabona, 4, 70125, Bari, Italy, and Dipartimento di Scienze Farmaceutiche, Università di Pisa, Via Bonanno, 6, 56126, Pisa, Italy

Received May 30, 2006

Some arylmethoxyphenyl derivatives were prepared as simplified structures of analogous arylpiperazines with high affinity toward dopaminergic D₂ and serotonergic 5-HT_{1A} receptors and inhibiting P-glycoprotein (P-gp). The compounds **5b** and **8b** displayed good P-gp inhibition activity measured as [³H]vinblastine transport inhibition in the Caco-2 cell monolayer and intracellular doxorubicin accumulation in MCF7/Adr cells by flow cytometry. Compounds **5b** and **8b** also inhibited, dose-dependently, ATP-ase activation induced by P-gp substrate vinblastine.

Introduction

Multidrug resistance (MDR) is a trend whereby tumor cells exposed to one cytotoxic agent develop cross-resistance to a range of structurally and functionally unrelated compounds.^{1–3} Different mechanisms can determine the development of MDR, such as (a) increased drug efflux from the cell by adenosine triphosphate (ATP) dependent transporters, (b) decreased drug uptake into the cell, (c) activation of detoxifying enzymes, and (d) defective apoptotic pathways.⁴ The MDR is due to the overexpression of P-glycoprotein (P-gp), a 170 KDa ATP-dependent membrane transporter that acts as a drug efflux pump. P-gp belongs to the ATP-binding cassette (ABC) family of transporters, currently numbering 49 members, that share sequence and structural homology.^{5,6} In cancerous tissues the expression of P-gp is highest in tumors derived from tissues that normally express P-gp, such as epithelial cells of the colon, kidney, adrenal, pancreas, and liver, resulting in the potential for resistance to some cytotoxic agents before chemotherapy is initiated.⁷

P-gp activity inhibition is a way of reversing MDR, and it has been extensively studied for more than 2 decades.⁸ Many agents modulating P-gp have been characterized, such as verapamil (Chart 1), cyclosporine-A, and several calmodulin antagonists, but all these compounds produced disappointing results in vivo because their low binding affinities necessitated the use of high doses, resulting in unacceptable toxicity.⁹ In addition, many of these chemosensitizers are substrates for other transporter and enzyme systems, resulting in unpredictable pharmacokinetic interaction in the presence of chemotherapy agents. To overcome these limitations, second-generation P-gp modulators have been developed, including (+)-verapamil (dexverapamil) and biricodar (Chart 1).^{10,11} These agents are more potent and less toxic than their predecessors, but they significantly inhibit the metabolism and excretion of chemotherapy, thus leading to unacceptable toxicity that has necessitated a chemotherapy dose reduction in clinical trials.^{12,13} In addition, many second-generation P-gp modulators also act as substrates for other transporters, particularly for those of the

ABC transporter family, the inhibition of which could lessen the ability of normal cells and tissues to protect themselves from cytotoxic agents.^{14,15} Third-generation P-gp inhibitors have been developed by SAR and combinatorial chemistry to overcome the limitation of the second-generation P-gp modulators.^{16,17} Third-generation P-gp inhibitors are in clinical development and include anthranilamide derivatives such as tariquidar and elacridar (Chart 1).¹⁸ This generation displayed a high potency for P-gp transporter but also inhibited breast cancer resistance protein (BCPR).¹⁹

An important physiological role of P-gp involves the blood–brain barrier (BBB), where P-gp is one critical selective component.²⁰ In fact, P-gp protects the central nervous system (CNS) from neurotoxicants and modulates brain penetration of a large number of drugs for treating CNS disorders.

While MDR and the mechanism of efflux from the CNS may appear to be different biological processes, the underlying molecular mechanism of action is common to both.^{21,22}

Results and Discussion

Recently, our group synthesized arylpiperazine derivatives as potential atypical antipsychotic drugs to obtain mixed D₂/5-HT_{1A} receptor affinity ligands^{23–25} (Chart 2A). As expected, these compounds displayed D₂ and 5-HT_{1A} K_i values from 6.0 to 1000 nM.²⁶ Moreover, for each compound the apparent permeability (*P*_{app}) as a predictive kinetic parameter for crossing BBB was determined.²⁷ Surprisingly, several arylpiperazine derivatives inhibited P-gp activity in the Caco-2 cell monolayer system in the presence of [³H]vinblastine as a specific P-gp substrate.

Since it is known that arylpiperazine moiety is responsible for dopaminergic and serotonergic receptor affinities, a new ligand series was prepared by removing the piperazine ring and linking the aryl group directly to the phenoxyalkyl nucleus (Chart 2B) in order to better understand the structure–activity relationships of P-gp inhibitors. For each compound, binding values obtained at D₂ and 5-HT_{1A} receptors were about 5000 nM (K_i).

The ability to inhibit [³H]vinblastine transport and the ATP-ase activity was determined for each compound.²⁸ Moreover, the compounds displaying P-gp inhibition activity were tested in the MCF-7/Adr cell line (human breast adenocarcinoma doxorubicin resistant), monitoring the ability of the tested compound to increase cell doxorubicin concentration by cytofluorimetric analysis.²⁹

* To whom correspondence should be addressed. For N.A.C.: phone, +39-080-5442727; fax, +39-080-5442231; e-mail: colabufo@farmchim.uniba.it. For S.R.: phone, 0502219582; fax, 0502219605; e-mail, rappsi@farm.unipi.it.

[†] Università degli Studi di Bari.

[‡] Università di Pisa.

Chart 1. P-gp Modulators

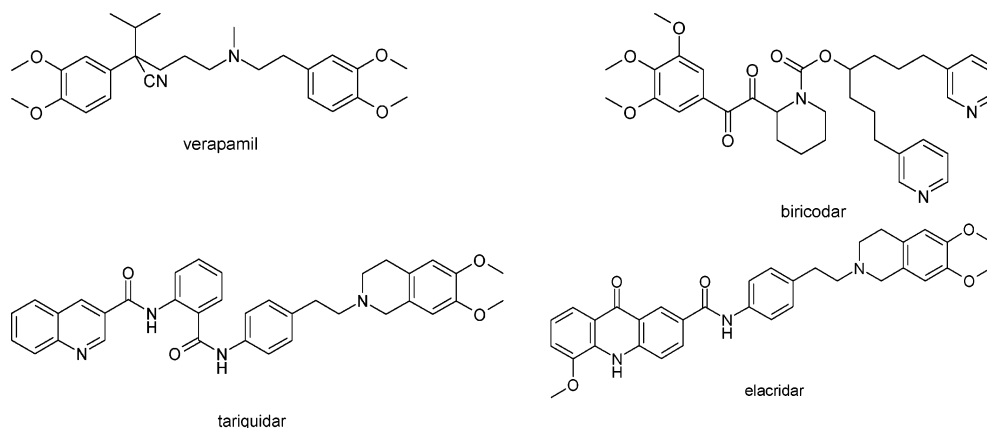


Chart 2. Arylpiperazinealkoxyphenol and Arylmethoxyphenyl Derivatives

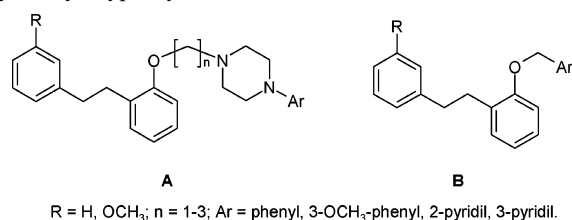


Table 1. Biological "in Vitro" Assays

compd	P-gp inhibition ^a	ATP-ase activation ^b
5a	100 ± 25	NA ^c
5b	27.6 ± 0.2	NA ^c
6a	125 ± 15	100 ± 10
6b	ND ^d	400 ± 25
7a	ND ^d	50.0 ± 5.0
7b	92.8 ± 5.5	NA ^c
8a	95.6 ± 10.0	200 ± 15
8b	17.2 ± 0.5	NA ^c
verapamil	20.0 ± 1.0	52.0 ± 7.5
elacridar	2.0 ^e	NA ^{c,e}

^a EC₅₀ ± SEM (μM) by three independent determinations (samples in triplicate). ^b Dose (μM) for obtaining the maximal inhibition. ^c No activation. ^d Not determined. ^e See ref 31.

The compounds **5a,b**, **6a,b**, **7a,b**, and **8a,b** were synthesized^{30,31} and tested in biological assays described above.

Compounds **6b** and **7a** were shown to be P-gp substrates because they were largely effluxed in the Caco-2 cell monolayer. These findings reflected the ATP-ase activation³² measured in the same cell line (EC₅₀ = 400 and 50 μM, respectively). All the other compounds that were not effluxed in the monolayer system were tested for inhibition of [³H]vinblastine basolateral-apical transport. The best results were obtained for compounds **5b** and **8b** (EC₅₀ = 27.6 and 17.2 μM, respectively), and their experimental values were superimposed onto those of the reference compound verapamil (Table 1).³² The elacridar P-gp inhibition value (EC₅₀ = 2.0 μM) was obtained in the MDR1-MDCKII monolayer cell system.³³ Moderate P-gp inhibition was obtained for compounds **5a**, **6a**, **7b**, and **8a** (EC₅₀ from 95.6 to 125 μM). The compounds displaying P-gp inhibition activity were consequently unable to activate the ATP-ase system linked to P-gp system. P-gp inhibitor verapamil activated ATP-ase because, as reported, it is a nontransported substrate.³³ Indeed, at low concentrations verapamil is a P-gp substrate, but at high concentrations, because of its high *P*_{app}, it penetrates the cell membrane and saturates the P-gp efflux system. To better correlate the P-gp inhibition of our compounds, we verified their ability to reduce ATP-ase activation by specific P-gp substrate

as vinblastine. ATP-ase activity was calibrated in Caco-2 cells, evaluating cell ATP availability time-dependently in the presence of 20 nM vinblastine.

As displayed in Figure 1A, the cell ATP depletion was about 50% of the basal level after 120 min for the untreated cells. In the presence of 20 μM P-gp inhibitors **5a**, **5b**, **7b**, **8a**, **8b**, the ATP increase was measured as a percentage value with respect to the basal level determined in the presence of 20 nM vinblastine at 120 min (Figure 1B). As expected, a higher increase was obtained for compounds **5b** and **8b**, which displayed the most potent ATP-ase inhibition (about 50% of cell ATP increase).

To better estimate the P-gp inhibition activity of compounds **5b** and **8b**, they were tested for their ability to increase doxorubicin accumulation in MCF-7/Adr where P-gp over-expression produces specific chemotherapeutic resistance.²⁸

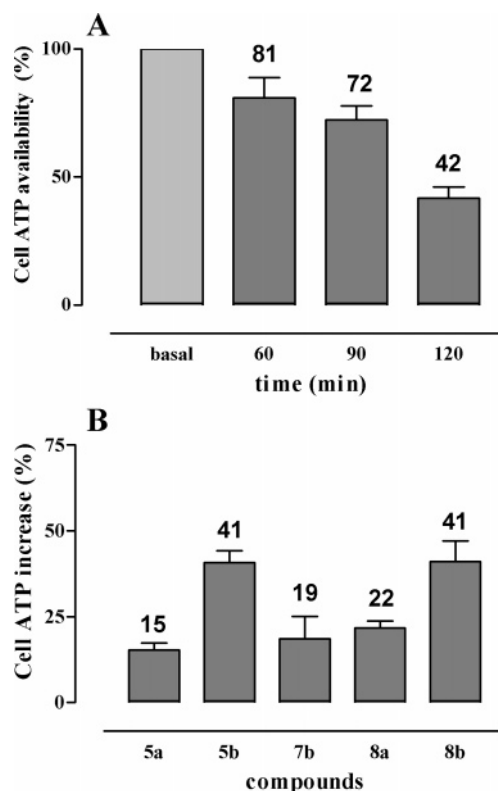


Figure 1. (A) Caco-2 cell ATP availability in the presence of 20 nM vinblastine. (B) Cell ATP increase with respect to the basal condition (20 nM vinblastine at 120 min) in the presence of P-gp inhibitors (20 μM).

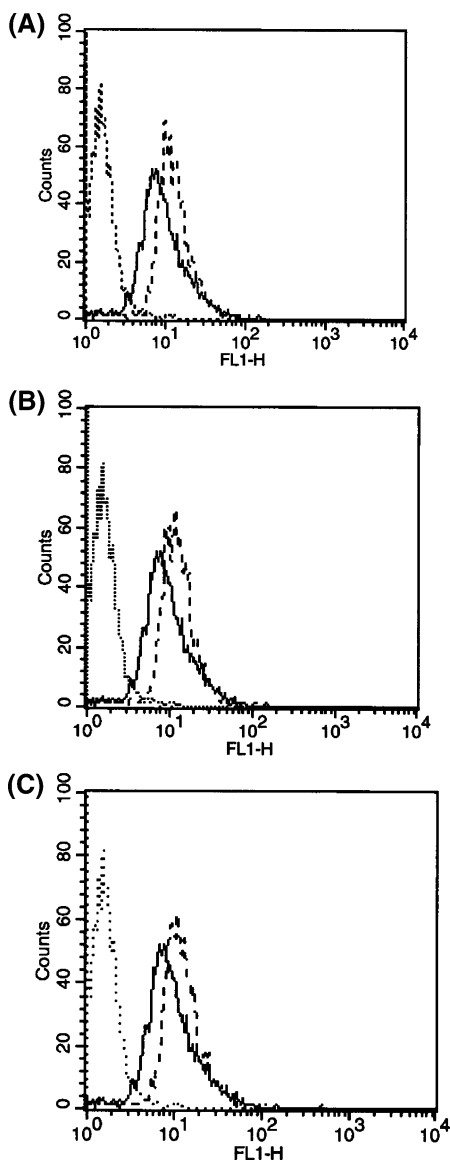


Figure 2. Flow cytometry analysis of verapamil (A), **5b** (B), and **8b** (C) in MCF7/Adr cells: (dotted line) autofluorescence; (solid line) doxorubicin alone (100%); (tract line) compound-dependent modulation of intracellular doxorubicin.

The modulation of doxorubicin intracellular accumulation elicited by compounds **5b** and **8b** was evaluated by flow cytometry, utilizing verapamil as a standard of P-gp inhibition (Figure 2). In the MCF7/Adr cells, doxorubicin was utilized at IC₅₀ concentration (50 μ M) for 1 day of exposure. The standard and the compounds **5b** and **8b** were utilized at 20 μ M for 2 h. The schedule of drug administration was as follows: the P-gp inhibitors for 2 h followed by two wash steps with complete medium and then followed by doxorubicin for 1 day. Fluorescence light emission from doxorubicin alone (solid line) was shifted to the right when P-gp inhibitor was added (tract line), indicating doxorubicin intracellular increase. As shown in Figure 2, the doxorubicin intracellular accumulation mediated by **5b** and **8b** was comparable to the corresponding effect displayed by verapamil.

Since the major limitation of many P-gp inhibitors such as verapamil is that they typically reverse MDR at a concentration that results in unacceptable toxicity, the cytotoxic effect at 48 h was determined for each compound. As depicted in Figure 3, at 100 μ M all compounds elicited cytotoxic activity from 8% to 25%. In contrast, verapamil showed 95% cytotoxic effect.

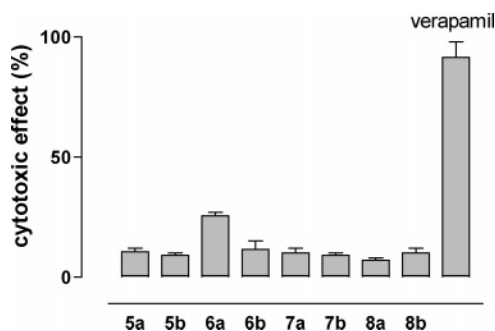


Figure 3. Cytotoxic effect at 48 h in MCF7/Adr cells. All compounds were tested at concentrations from 1 to 100 μ M. The cytotoxic effect at 100 μ M are reported for each compound.

Therefore, although verapamil and **5b** and **8b** displayed comparable P-gp inhibition, our compounds were devoid of cytotoxic activity.

Conclusions

These preliminary results showed that arylmethoxyphenyl derivatives modulated P-gp activity and that the aryl moiety characterized the intrinsic activity. In particular, 2-pyridil derivative **5b** was a P-gp inhibitor while the corresponding 3-pyridil **6b** was a P-gp substrate. Similarly, the 3-methoxyphenyl derivative **8b** displayed P-gp inhibition activity while the corresponding unsubstituted derivative **7a** was a P-gp substrate. Furthermore, the best P-gp inhibitors, **5b** and **8b**, displayed a potency similar to that of verapamil; however, the latter was a P-gp nontransported substrate.

In contrast, although compounds **5b** and **8b** displayed P-gp inhibition activity that was 10-fold less potent than that of elacridar, these compounds were, like elacridar, devoid of intrinsic activity. In addition, and more importantly, the structures of our compounds are simpler than that of elacridar, meaning that structure–activity relationship studies regarding P-gp inhibition can be more easily carried out with our compounds.

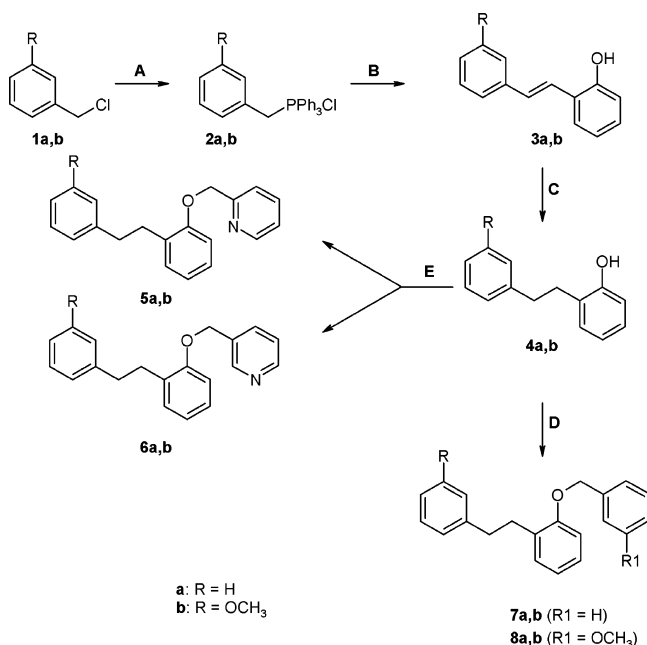
New aryl derivatives of the arylmethoxyphenyl class will be developed both to improve the P-gp inhibition effect and to better understand the structural requirements responsible for this action, which does not cause substrate efflux.

Chemistry

Final compounds were prepared by alkylation of phenol derivatives **4a,b** with benzyl chloride in the presence of KOH to obtain compounds **7a,b** and with 3-methoxybenzyl chloride to obtain compounds **8a,b**. Moreover, the same intermediates **4a,b** give, in the presence of 2- or 3-(chloromethyl)pyridine, compounds **5a,b** and **6a,b**, respectively (Scheme 1). The phenol derivatives **4a,b** were synthesized as previously described.^{30,31} The substituted benzylchlorides **1a,b** were converted to the phosphonium salts **2a,b**, which were submitted to Wittig reactions with salicylbenzaldehyde to give stylbenes **3a,b** as mixtures of cis and trans isomers. The subsequent catalytic hydrogenation of **3a,b** afforded the phenol derivatives **4a,b**.

Experimental Section

Melting points were determined on a Kofler hot-stage apparatus and are uncorrected. ¹H NMR spectra of all compounds were obtained with a Gemini 200 spectrometer operating at 200 MHz,

Scheme 1^a

^a Reagents: (A) PPh₃, CH₃CN; (B) salicylaldehyde, DBU (1,8-diazabicyclo[5.4.0]undec-7-ene), CH₃CN; (C) H₂, Pd/C 10%; (D) benzyl- or 3-OCH₃-benzylchloride, KOH, DMSO; (E) 2-chloro- or 3-(chloromethyl)pyridine, KOH.

in a ~2% solution of CDCl₃. Analytical TLC experiments were carried out on 0.25 mm layer silica gel plates containing a fluorescent indicator; spots were detected under UV light (254 nm). Column chromatography was performed using 70–230 mesh silica gel. Mass spectra were detected with a Hewlett Packard 5988A spectrometer. Evaporations were made in vacuo (rotating evaporator). Na₂SO₄ was always used as the drying agent. Elemental analyses were performed in our analytical laboratory, and the results agreed with the theoretical values to within ±0.4%.

Benzyl(chloro)triphenylphosphorane (2a). A stirred solution of benzyl chloride **1a** (2.88 g, 31.6 mmol) in CH₃CN (20 mL) was treated with PPh₃ (8.57 g, 32.7 mmol), and the mixture was vigorously stirred, refluxed for 12 h, and then evaporated. The crude product was purified by crystallization from CHCl₃/Et₂O, affording **2a** (11.7 g, 30.02 mmol, 95% yield) as a white solid: mp 324–326 °C. MS *m/z* 353 (M⁺ – Cl, 100). ¹H NMR: δ 5.45 (d, 2H, *J* = 14.5 Hz, CH₂P), 7.07–7.23 (m, 5H, Ar), 7.56–7.78 (m, 15H, Ph). Anal. (C₂₅H₂₂PCl) C, H.

3-Methoxybenzyl(chloro)triphenylphosphorane (2b). Compound **2b** was synthesized from **1b** (5 g, 32 mmol) and PPh₃ (9.20 g, 33.93 mmol) in CH₃CN (20 mL) following the same procedure as described above for the preparation of **2a**. The crude residue was purified by precipitation from CHCl₃/Et₂O to give compound **2b** (13.14 g, 31.36 mmol, 98% yield). MS *m/z* 383 (M⁺ – Cl, 28). ¹H NMR: δ 3.53 (s, 3H, OCH₃), 5.44 (d, 2H, *J* = 16 Hz, CH₂), 6.60–6.77 (m, 3H, Ar), 7.02 (t, 1H, *J* = 7.6 Hz, Ar), 7.11–7.21 (m, 15H, Ph). Anal. (C₂₆H₂₄POCl) C, H.

2-[(E/Z)-2-Phenylethyl]phenol (3a). A solution of 1,8-diazabicyclo[5.4.0]undec-7-ene (DBU) (1.17 g, 7.7 mmol), salicylaldehyde (0.9 g, 7.45 mmol), and benzyltriphenylphosphonium chloride **2a** (2.89 g, 7.45 mmol) in CH₃CN (12 mL) was stirred for 12 h under reflux. Then the solvent was removed and the residue was diluted with CHCl₃ and washed with water, 1 N HCl, and brine. The organic layer was dried and evaporated to afford a mixture of *cis*- and *trans*-stilbene **3a** as an oil, which was submitted to the subsequent reaction without any further purification.³¹ MS (*m/z*) 196 (M⁺, 39). ¹H NMR: δ 6.90–7.33 (m, 11H, Ar, CH=CH).

2-[(E/Z)-2-(3-Methoxyphenyl)vinyl]phenol (3b). Compound **3b** was synthesized from **2b** (2 g, 4.78 mmol) and salicylaldehyde (0.6 g, 4.78 mmol) in CH₃CN (15 mL) following the same procedure as described above for the preparation of **3a**.³¹ MS (*m/z*) 226 (M⁺,

48), 195 (M⁺ – OCH₃, 12). ¹H NMR: δ 3.81 (s, 3H, OMe), 6.55–7.23 (m, 10H, Ar, CH=CH).

2-(2-Phenylethyl)phenol (4a). The mixture of *cis*- and *trans*-stilbene **3a** (2.70 g, 13.80 mmol) was hydrogenated in EtOH (70 mL) in the presence of 10% Pd–C (225 mg, 2.12 mmol) for 12 h. Then the catalyst was filtered off, and the solution was evaporated to dryness. The residual material was purified by column chromatography, eluting with CHCl₃ to afford compound **4a** (1.01 g, 5.10 mmol, yield 37%).²⁹ ¹H NMR: δ 2.87–2.96 (s, 4H, CH₂CH₂), 4.85 (br s, OH), 6.74–6.90 (m, 2H, Ar), 7.05–7.13 (m, 2H, Ar), 7.19–7.30 (m, 5H, Ar).

2-[2-(3-Methoxyphenyl)ethyl]phenol (4b). The mixture of *cis*- and *trans*-stilbene **3b** (1.30 g, 5.75 mmol) was hydrogenated in EtOH (30 mL) in the presence of 10% Pd–C (177 mg, 1.67 mmol) for 12 h. Then the catalyst was filtered off and the solution was evaporated to dryness. The residual material was purified by column chromatography, eluting with CHCl₃ to afford compound **4b** (0.59 g, 2.58 mmol, yield 45%). MS *m/z* 228 (M⁺, 28). ¹H NMR: δ 2.93 (s, 4H, CH₂CH₂), 3.79 (s, 3H, OCH₃), 4.76 (br s, OH), 6.73–6.92 (m, 4H, Ar), 7.06–7.28 (m, 4H, Ar).

2-[[2-(2-Phenylethyl)phenoxy]methyl]pyridine (5a). A solution of 2-(2-phenylethyl)phenol **4a** (225 mg, 1.14 mmol) in a small amount of DMSO (2 mL) was added to a solution of KOH (174.4 mg, 3.11 mmol) in DMSO (2.5 mL). Stirring was continued over 15 min at room temperature. Then a solution 2-(chloromethyl)pyridine hydrochloride (187 mg, 1.14 mmol) in DMSO (2 mL) was added dropwise to the solution of potassium 2-(2-phenylethyl)benzenolate. The suspension was stirred at room temperature for 12 h. Then it was diluted with AcOEt and washed with water and brine. The organic layer was dried and concentrated. The crude product was chromatographed on a silica gel column, eluting with CHCl₃/Et₂O (8:2) to give **5a** as an oil, which was transformed to hydrochloride and crystallized from *i*-PrOH (230 mg, 0.71 mmol, 62% yield): mp 116–118 °C. MS *m/z* 289 (M⁺, 57), 198 (M⁺ – CH₂Py, 24). ¹H NMR: δ 2.91–3.07 (m, 4H, CH₂CH₂), 5.69 (s, 2H, CH₂), 6.93–7.03 (m, 2H, Ar), 7.12–7.27 (m, 7H, Ar), 7.84 (t, 1H, *J* = 6.7 Hz, Py), 7.94 (d, 1H, *J* = 7.8 Hz, Py), 8.37 (t, 1H, *J* = 7.8 Hz, Py), 8.72 (d, 1H, *J* = 5.2 Hz, Py). ¹³C NMR: δ 154.78, 153.65, 145.47, 141.93, 140.79, 130.53, 128.52, 128.36, 127.74, 126.03, 125.46, 124.77, 122.43, 112.06, 64.98, 36.64, 32.11. Anal. (C₂₀H₁₉NO·HCl) C, H, N.

2-[[2-(2-(3-Methoxyphenyl)ethyl)phenoxy]methyl]pyridine (5b). Compound **5b** was synthesized from **4b** (200 mg, 0.88 mmol), KOH (174.4 mg, 3.11 mmol), and 2-(chloromethyl)pyridine hydrochloride (136 mg, 0.88 mmol) following the same procedure as described above for the preparation of **5a**. The crude product was chromatographed on a silica gel column, eluting with hexane/Et₂O (1:1) to give **5b** (150 mg, 0.47 mmol, 53% yield) as an oil. MS *m/z* 319 (M⁺, 65), 211 (M⁺ – OCH₂Ar, 55). ¹H NMR: δ 2.89–3.10 (m, 4H, CH₂CH₂), 3.78 (s, 3H, OCH₃), 5.25 (s, 2H, CH₂), 6.74–6.93 (m, 5H, Ar), 7.16–7.27 (m, 4H, Ar, Py), 7.55 (d, 1H, *J* = 7.8 Hz, Py), 7.74 (t, 1H, *J* = 7.8 Hz, Py), 8.62 (m, 1H, Py). ¹³C NMR: δ 160.26, 158.37, 156.84, 149.83, 144.69, 137.56, 131.08, 130.84, 129.93, 128.05, 123.24, 121.66, 114.94, 112.36, 111.90, 71.28, 55.89, 37.27, 33.46. Anal. (C₂₁H₂₁NO₂) C, H, N.

3-[[2-(2-Phenylethyl)phenoxy]methyl]pyridine (6a). Compound **6a** was synthesized from **4a** (225 mg, 1.14 mmol) and 3-(chloromethyl)pyridine hydrochloride (187 mg, 1.14 mmol) following the same procedure as described above for the preparation of **5a**. The crude product was purified by transformation to hydrochloride and crystallization from EtOH to give **6a** (160 mg, 0.50 mmol, 44% yield) as a white solid: mp 146–148 °C. MS *m/z* 318 (M⁺, 92), 211 (M⁺ – OCH₂Py, 47). ¹H NMR: δ 2.88–3.02 (m, 4H, CH₂CH₂), 5.15 (s, 2H, CH₂), 6.81 (d, 1H, *J* = 8.2 Hz, Ar), 6.97–7.10 (m, 3H, Ar), 7.15–7.25 (m, 5H, Ar), 7.90–7.97 (m, 1H, Py), 8.36 (d, 1H, *J* = 7.8 Hz, Py), 8.73–8.78 (m, 2H, Py). ¹³C NMR: δ 155.20, 143.44, 141.82, 140.16, 139.47, 138.56, 130.64, 128.54, 128.34, 127.52, 126.85, 125.96, 122.22, 111.86, 65.93, 36.70, 32.04. Anal. (C₂₀H₁₉NO·HCl) C, H, N.

3-[[2-(2-(3-Methoxyphenyl)ethyl)phenoxy]methyl]pyridine (6b). Compound **6b** was synthesized from **4b** (200 mg, 0.88 mmol) and

3-(chloromethyl)pyridine hydrochloride (144 mg, 0.88 mmol) following the same procedure as described above for the preparation of **5a**. The crude product was transformed in hydrochloride and crystallized from *i*-PrOH/*i*-Pr₂O to give **6b** (125 mg, 0.35 mmol, 79% yield) as a white solid: mp 147–149 °C. MS (*m/z*) 319 (M⁺, 98), 212 (M⁺ – OCH₂Py, 100). ¹H NMR: δ 2.88–2.98 (m, 4H, CH₂CH₂), 3.71 (s, 3H, OCH₃), 5.16 (s, 2H, CH₂), 6.58 (s, 1H, Ar), 6.65–6.70 (m, 2H, Ar), 6.82 (d, 1H, *J* = 8.4 Hz, Ar), 7.00 (t, 1H, *J* = 7.2 Hz, Ar), 7.10–7.24 (m, 3H, Ar), 7.91–7.97 (m, 1H, Py), 8.38 (d, 1H, *J* = 8.2 Hz, Py), 8.75 (d, 1H, *J* = 5.4 Hz, Py), 8.83 (s, 1H, Py). ¹³C NMR: δ 159.61, 155.24, 143.47, 139.41, 138.61, 130.69, 130.58, 129.36, 127.60, 126.87, 122.35, 121.04, 114.45, 111.90, 111.32, 65.94, 55.29, 36.77, 31.89. Anal. (C₂₁H₂₁NO₂·HCl) C, H, N.

1-(Benzyloxy)-2-(2-phenylethyl)benzene (7a). A solution of 2-(2-phenylethyl)phenol **4a** (200 mg, 1.01 mmol) in a small amount of DMSO (2 mL) was added to a solution of KOH (174.4 mg, 3.11 mmol) in DMSO (2.5 mL). Stirring was continued over 15 min at room temperature. Then a solution of benzyl chloride (128 mg, 1.01 mmol) in DMSO (2 mL) was added dropwise to the solution of potassium 2-(2-phenylethyl)benzenolate. The suspension was stirred at room temperature for 12 h. Then it was diluted with AcOEt and washed with water and brine. The organic layer was dried and concentrated. The resulting residue was purified by chromatography on a silica gel column, eluting with hexane/AcOEt (8:2) to give **7a** (87 mg, 0.31 mmol, 30% yield) as a colorless oil. MS *m/z* 288 (M⁺, 20), 197 (M⁺ – CH₂Ph, 73). ¹H NMR: δ 2.88–3.07 (m, 4H, CH₂CH₂), 5.13 (s, 2H, CH₂O), 6.89–6.98 (m, 2H, Ar), 7.16–7.52 (m, 12H, Ar). ¹³C NMR: δ 157.42, 143.20, 138.23, 131.44, 130.82, 129.25, 128.96, 128.51, 127.92, 126.45, 121.48, 112.50, 70.75, 37.25, 33.71. Anal. (C₂₁H₂₀O) C, H.

1-(Benzyloxy)-2-[2-(3-methoxyphenyl)ethyl]benzene (7b). Compound **7b** was synthesized from **4b** (200 mg, 0.88 mmol) and benzyl chloride (110 mg, 0.88 mmol) following the same procedure as described above for the preparation of **7a**. The crude product was purified by column chromatography, eluting with hexane/AcOEt (9:1) to afford **7b** (137 mg, 0.43 mmol, 49% yield) as an oil. MS *m/z* 318 (M⁺, 85), 212 (M⁺ – CH₂Ph, 33). ¹H NMR: δ 2.94–3.09 (m, 4H, CH₂CH₂), 3.80 (s, 3H, OCH₃), 5.16 (s, 2H, CH₂O), 6.79–6.88 (m, 3H, Ar), 6.95–7.02 (m, 2H, Ar), 7.22–7.30 (m, 1H, Ar), 7.40–7.56 (m, 7H, Ar). ¹³C NMR: δ 159.61, 156.67, 154.31, 144.15, 137.50, 130.64, 130.16, 129.27, 128.62, 127.87, 127.30, 121.0, 120.79, 114.09, 111.68, 111.43, 69.97, 55.22, 36.66, 33.10. Anal. (C₂₂H₂₂O₂) C, H.

1-[3-(Methoxybenzyl)oxy]-2-(2-phenylethyl)benzene (8a). Compound **8a** was synthesized from **4a** (200 mg, 1.01 mmol) and 3-methoxybenzyl chloride (157 mg, 1.01 mmol) following the same procedure as described above for the preparation of **7a**. The crude product was chromatographed on a silica gel column, eluting with hexane/AcOEt (9:1) to give **8a** (213 mg, 0.67 mmol, 66% yield) as an oil. MS *m/z* 318 (M⁺, 96), 211 (M⁺ – CH₂Ar, 55). ¹H NMR: δ 2.90–2.98 (m, 4H, CH₂CH₂), 3.80 (s, 3H, OCH₃), 5.08 (s, 2H, CH₂), 6.86–6.94 (m, 3H, Ar), 7.02–7.09 (m, 2H, Ar), 7.12–7.31 (m, 8H, Ar). ¹³C NMR: δ 159.22, 155.98, 141.85, 138.50, 129.51, 129.02, 128.07, 127.69, 126.65, 125.17, 120.17, 118.75, 112.76, 111.97, 111.08, 69.20, 54.69, 35.92, 32.49. Anal. (C₂₂H₂₂O₂) C, H.

1-[3-(Methoxybenzyl)oxy]-2-[2-(3-methoxyphenyl)ethyl]benzene (8b). Compound **8b** was synthesized from **4b** (200 mg, 0.88 mmol) and 3-methoxybenzyl chloride (136 mg, 0.88 mmol) following the same procedure as described above for the preparation of **7a**. The crude product was chromatographed on a silica gel column, eluting with hexane/Et₂O (8:2) to give **8b** (198 mg, 0.57 mmol, 65% yield) as an oil. MS *m/z* 348 (M⁺, 25). ¹H NMR: δ 2.85–3.01 (m, 4H, CH₂CH₂), 3.74 (s, 3H, OCH₃), 3.79 (s, 3H, OCH₃), 5.07 (s, 2H, CH₂), 6.71–6.80 (m, 2H, Ar), 6.85–6.93 (m, 3H, Ar), 7.02–7.05 (m, 2H, Ar), 7.13–7.22 (m, 3H, Ar), 7.25–7.35 (m, 2H, Ar). ¹³C NMR: δ 160.59, 160.33, 157.35, 144.78, 139.83, 131.37, 130.84, 130.29, 129.89, 127.94, 121.68, 121.51, 120.08, 114.81, 114.09, 113.38, 112.50, 112.12, 70.62, 55.98, 55.87, 37.30, 33.62. Anal. (C₂₃H₂₄O₃) C, H.

Biological Section. Materials and Methods. Caco-2 cells were obtained from Dr. Aldo Cavallini and Dr. Caterina Messa from Laboratory of Biochemistry, National Institute for Digestive Diseases, “S. de Bellis”, Bari, Italy. MultiScreen Caco-2 plate system with 96 wells was purchased from Millipore Corporation, Life Science Division, Danvers, MA. [³H]Vinblastine was purchased from Amersham Life Sciences (Arlington Heights, IL). Verapamil hydrochloride was purchased from Tocris Bioscience, Bristol, U.K.

[³H]Vinblastine Transport Inhibition. Caco-2 cells were seeded onto Multiscreen plates with 20 000 cells/well for 10 days, measuring the integrity of the cell monolayers by trans-epithelial electrical resistance (TEER, Ω·cm²) with an epithelial voltohmmeter (Millicell-ERS; Millipore, Billerica, MA). Mature Caco-2 cell monolayer exhibited a TEER of >800 Ω·cm² prior to use in transport experiments. Transport experiments for tested compounds were carried out as described by Taub et al.²⁸

To the basolateral (BL) compartment in each well, in the absence and in the presence of P-gp inhibitors (from 200 nM to 400 μM), was added 20 nM [³H]vinblastine for 120 min at 37 °C, and its appearance in the apical (AP) compartment was monitored. At 120 min, a 20 μL sample was taken from the donor compartment to determine the concentration of radioligand remaining in the donor chamber at the end of the experiment. Samples were analyzed using a LS6500 Beckman counter. For each compound, [³H]vinblastine transport inhibition was calculated as the radioactivity difference between the radioligand in the presence and absence of compound. These differences were expressed as an inhibition percentage at a single drug concentration.

Cell ATP availability Assay. This experiment was performed as reported in the technical sheet of the ATPlite 1step kit for luminescence ATP detection using Victor3, from PerkinElmer Life Sciences.³²

Intracellular Doxorubicin Accumulation. The modulation of doxorubicin intracellular accumulation by **5b** and **8b** was evaluated by flow cytometry, utilizing verapamil as the standard of P-gp inhibition.²⁹ In all experiments, the various drug solvents (ethanol, DMSO) were added to each control to evaluate the solvent influence. In MCF7/Adr cells, doxorubicin was utilized at IC₅₀ concentration (50 μM) for 1 day of exposure, and the standard and the newly synthesized P-gp compounds were utilized at 20 μM for 2 h. The schedule of drug administration was the P-gp inhibitors for 2 h, followed, after two wash steps with complete medium, by doxorubicin for 1 day. After incubation, the cell media were removed and trypsin–EDTA was used to detach the cells from the plates. Cells were harvested, washed twice in ice-cold PBS (pH 7.4), and placed on ice (less than 1 h) until analysis. Fluorescence measurements of individual cells were performed with a Becton-Dickinson FACScan equipped with an ultraviolet argon laser. Analysis was gated to include single cells on the basis of forward and side light scatter and was based on the acquisition of data from 5000 cells. The log of the fluorescence was collected and displayed as single-parameter histograms. The mean fluorescence intensity of doxorubicin in the doxorubicin-treated cells, arbitrarily established as 100%, represented the positive control (MF_{PC}). The autofluorescence of untreated cells, arbitrarily established as 0%, was the negative control (MF_{NC}). The doxorubicin mean fluorescence intensity of doxorubicin in the verapamil or of other newly synthesized agents plus doxorubicin-treated cells was MF_S. The amount of doxorubicin in the samples was obtained by the following formula:

$$\% \text{ doxorubicin in samples} = \frac{\text{MF}_S - \text{MF}_{\text{NC}}}{\text{MF}_{\text{PC}} - \text{MF}_{\text{NC}}} \times 100$$

Cytotoxicity Assay. The assay was performed using the Cyto-Tox-One kit from the Promega Corp. (Madison, WI) as reported in a previous paper.³⁴ Cell death was determined as the release of lactate dehydrogenase (LDH) into the culture medium. The percentage of cytotoxicity was calculated relative to the LDH release from total lysis of cells in untreated control. It is assumed here that the drug-treated wells and the control wells contained the same total

number of cells (dead plus alive cells) at the end of the treatment period. Therefore, the cytotoxic effect of tested compounds was unaffected by any underestimation of cytotoxicity that could occur because of decreased total number of cells in the treated samples compared to that of the untreated control. Cells were seeded into 96-well plates for optical performance in the fluorescent cell-based assay in 100 μ L of complete medium in the presence or absence of different concentrations of test compounds. The plate was incubated for 24 h in a humidified atmosphere of 5% CO₂ at 37 °C, and then 100 μ L of the substrate mix in assay buffer was added. The 10 μ L lysis solution was added to untreated wells in order to estimate total LDH. Plates were kept protected from light for 10 min at room temperature, and 50 μ L of stop solution was added to all wells. The fluorescence was recorded using a LS55 luminescence spectrometer from PerkinElmer with a 560 nm excitation wavelength and a 590 nm emission wavelength. The cytotoxicity percentage was estimated as follows:

$$\frac{(\text{LDH in medium of treated cells}) - (\text{culture medium background})}{(\text{total LDH in untreated cells}) - (\text{culture medium background})} \times 100$$

Acknowledgment. We thank Dr. Amalia Azzariti and Dr. Angelo Paradiso, from Clinical Experimental Oncology Laboratory, National Cancer Institute, Bari, Italy, for providing flow cytometry results.

Supporting Information Available: Results from elemental analysis. This material is available free of charge via the Internet at <http://pubs.acs.org>.

References

- Bates, E. S.; Robey, R.; Knutsen, T.; Honjo, Y.; Litman, T.; Dean, M. New ABC transporters in multi-drug resistance. *Emerging Ther. Targets* **2000**, *4*, 561–580.
- Gottesman, M. M.; Fojo, T.; Bates, S. E. Multidrug resistance in cancer: role of ATP-dependent transporters. *Nat. Rev. Cancer* **2002**, *2*, 48–58.
- Ambudkar, S. V.; Dey, S.; Hrycyna, C. A.; Ramachandra, M.; Pastan, I.; Gottesman, M. M. Biochemical, cellular, and pharmacological aspects of the multidrug transporter. *Annu. Rev. Pharmacol. Toxicol.* **1999**, *39*, 361–398.
- Thomas, H.; Coley, H. M. Overcoming multidrug resistance in cancer: an update on the clinical strategy of inhibiting P-glycoprotein. *Cancer Control* **2003**, *10*, 159–164.
- Leslie, E. M.; Deeley, R. G.; Cole, S. P. C. Multidrug resistance proteins: role of P-glycoprotein MRP1, MRP2, and BCRP (ABCG2) in tissue defense. *Toxicol. Appl. Pharmacol.* **2005**, *204*, 216–237.
- Schneider, E.; Paul, D.; Ivy, P.; Cowan, K. H. Multidrug resistance. *Cancer Chemother. Biol. Response Modif.* **1999**, *18*, 152–177.
- Fardel, O.; Lecœur, V.; Guillouzo, A. The P-glycoprotein multidrug transporter. *Gen. Pharmacol.* **1996**, *39*, 361–398.
- Ferry, D. R.; Traunecker, H.; Kerry, D. J. Clinical trials of P-glycoprotein reversal in solid tumours. *Eur. J. Cancer* **1996**, *32A*, 1070–1081.
- Krishna, R.; Mayer, L. D. Multidrug resistance (MDR) in cancer. Mechanisms, reversal using modulators of MDR and the role of MDR modulators in influencing the pharmacokinetics of anticancer drugs. *Eur. J. Pharmacol. Sci.* **2000**, *11*, 265–283.
- te Boekhorst, P. A.; van Kapel, J.; Schoester, M.; Sonneveld, P. Reversal of typical multidrug resistance by cyclosporin and its non-immunosuppressive analogue SDZ PSC 833 in Chinese hamster ovary cells expressing the mdr1 phenotype. *Cancer Chemother. Pharmacol.* **1992**, *30*, 238–242.
- Twentyman, P. R.; Bleeche, N. M. Resistance modification by PSC-833, a novel non-immunosuppressive cyclosporin. *Eur. J. Cancer* **1991**, *27*, 1639–1642.
- Advani, R.; Saba, H. I.; Tallman, M. S.; Rowe, J. M.; Wiernik, P. H.; Ramek, J.; Dugan, K.; Lum, B.; Villena, J.; Davis, E.; Paietta, E.; Litchman, M.; Sicik, B. I.; Greenberg, P. L. Treatment of refractory and relapsed acute myelogenous leukaemia with combination chemotherapy plus the multidrug resistance modulator PSC 833 (Valspodar). *Blood* **1999**, *93*, 787–795.
- Chico, I.; Kang, M. H.; Bergan, R.; Abraham, J.; Bakke, S.; Meadows, B.; Rutt, A.; Robey, R.; Choyke, P.; Merino, M.; Goldspiel, B.; Smith, T.; Steinberg, S.; Figg, W. D.; Fpjo, T.; Bates, S. Phase I study of infusional paclitaxel in combination with the P-glycoprotein antagonist PSC 833. *J. Clin. Oncol.* **2001**, *19*, 832–842.
- Yanagisawa, T.; Newman, A.; Coley, H.; Renshaw, J.; Pinkerton, C. R.; Pritchard-Jones, K. BIRICODAR (VX-710; Incel): an effective chemosensitizer in neuroblastoma. *Br. J. Cancer* **1999**, *80*, 1190–1196.
- Rowinsky, E. K.; Smith, L.; Wang, Y. M.; Chatuverdi, P.; Villalona, M.; Campbell, E.; Aylesworth, C.; Eckhardt, S. G.; Hammond, L.; Kraynak, M.; Drengler, R.; Stephenson, J., Jr.; Harding, M. W.; Von Hoff, D. D. Phase I and pharmacokinetic study of paclitaxel in combination with biricodar, a novel agent that reverse multidrug resistance conferred by overexpression of both MDR1 and MRP. *J. Clin. Oncol.* **1998**, *16*, 2964–2976.
- Wandel, C.; Kim, R. B.; Kajiji, S.; Guengerich, P.; Wilkinson, G. R.; Wood, A. J. P-glycoprotein and cytochrome P-450 3A inhibition: dissociation of inhibitory potencies. *Cancer Res.* **1999**, *59*, 3944–3948.
- Dantzig, A. H.; Shepard, R. L.; Law, K. L.; Tabas, L.; Pratt, S.; Gillespie, J. S.; Binkley, S. N.; Kuhfeld, M. T.; Starling, J. J.; Wrighton, S. A. Selectivity of the multidrug resistance modulator, LY335979, for P-glycoprotein and effect on cytochrome P-450 activities. *J. Pharmacol. Exp. Ther.* **1999**, *290*, 854–862.
- Mistry, P.; Stewart, A. J.; Dangerfield, W.; Okiji, S.; Liddle, C.; Bootle, D.; Plumb, J. A.; Templeton, D.; Charlton, P. In vitro and in vivo reversal of P-glycoprotein-mediated multidrug resistance by a novel potent modulator, XR9576. *Cancer Res.* **2001**, *61*, 749–758.
- Kruijtzter, C. M. F.; Beijnen, J. H.; Rosing, H.; ten Bokkel Huinink, W. W.; Schot, M.; Jewell, R. C.; Paul, E. M.; Schellens, J. H. M. Increased oral bioavailability of topotecan in combination with the breast cancer resistance protein and P-glycoprotein inhibitor GF120918. *J. Clin. Oncol.* **2002**, *20*, 2943–2950.
- Breedveld, P.; Beijnen, J. H.; Schellens, J. H. M. Use of P-glycoprotein and BCRP inhibitors to improve oral bioavailability and CNS penetration of anticancer drugs. *Trends Pharmacol. Sci.* **2006**, *27*, 17–24.
- Fromm, M. F. P-glycoprotein: a defense mechanism limiting oral bioavailability and CNS accumulation of drugs. *Int. J. Clin. Pharmacol. Ther.* **2000**, *38*, 69–74.
- Loscher, W.; Potschka, H. Role of drug efflux transporters in the brain for drug disposition and treatment of brain diseases. *Prog. Neurobiol.* **2005**, *76*, 22–76.
- Perrone, R.; Berardi, F.; Colabufo, N. A.; Tortorella, V.; Fiorentini, F.; Olgiati, V.; Vanotti, E.; Govoni, S. Mixed 5-HT_{1A}/D-2 activity of a new model of arylpiperazines: 1-aryl-4-[3-(1,2-dihydronaphthalen-4-yl)-n-propyl]piperazines. 1. Synthesis and structure–activity relationships. *J. Med. Chem.* **1994**, *37*, 99–104.
- Perrone, R.; Berardi, F.; Colabufo, N. A.; Leopoldo, M.; Tortorella, V.; Fiorentini, F.; Olgiati, V.; Ghiglieri, A.; Govoni, S. High affinity and selectivity on 5-HT_{1A} receptor of 1-aryl-4-[(1-tetralin)alkyl]piperazines. 2. *J. Med. Chem.* **1995**, *38*, 942–949.
- Perrone, R.; Berardi, F.; Colabufo, N. A.; Leopoldo, M.; Tortorella, V.; Fornaretto, M. G.; Caccia, C.; McArthur, R. A. Structure–activity relationship studies on the 5-HT_{1A} receptor affinity of 1-phenyl-4-[ω -(α - or β -tetralinyl)alkyl]piperazines. 4. *J. Med. Chem.* **1996**, *38*, 4928–4934.
- Unpublished results.
- Artursson, P.; Karlsson, J. Correlation between oral drug absorption in humans and apparent drug permeability coefficients in human intestinal epithelial (Caco-2) cells. *Biochem. Biophys. Res. Commun.* **1991**, *175*, 880–885.
- Taub, M. E.; Podila, L.; Almeida, I. Functional assessment of multiple P-glycoprotein (P-gp) probe substrate: influence of cell line and modulator concentration on P-gp activity. *Drug Metab. Dispos.* **2005**, *33*, 1679–1687.
- Azzariti, A.; Colabufo, N. A.; Berardi, F.; Porcelli, L.; Niso, M.; Simone, M. G.; Perrone, R.; Paradiso, A. Cyclohexylpiperazine derivative PB28, a sigma-2 agonist and sigma-1 antagonist receptor activity, inhibits cell growth, modulates P-glycoprotein and synergizes with anthracyclines in breast cancer. *Mol. Cancer Ther.* **2006**, *5*, 1807–1816.
- Kikumoto, R.; Hara, H.; Ninomiya, K.; Osakabe, M.; Sugano, M.; Fukami, H.; Tamao, Y. Syntheses and platelet aggregation inhibitory and antithrombotic properties of [2-[(ω -aminoalkoxy)phenyl] ethyl]-benzenes. *J. Med. Chem.* **1990**, *33*, 1818–1823.
- Kikumoto, R.; Tobe, A.; Fukami, H.; Egawa, M. Substituted (ω -aminoalkoxy)stilbene derivatives as a new class of anticonvulsants. *J. Med. Chem.* **1984**, *27*, 645–649.

- (32) Kangas, L.; Grönroos, M.; Nieminem, A. L. Bioluminescence of cellular ATP: a new method for evaluating agents in vitro. *Med. Biol.* **1984**, *62*, 338–343.
- (33) Polli, J. W.; Wring, S. A.; Humphreys, J. E.; Huang, L.; Morgan, J. B.; Webster, L. O.; Serabjit-Singh, C. S. Rational use of in vitro P-glycoprotein assays in drug discovery. *J. Pharmacol. Exp. Ther.* **2001**, *299*, 620–628.
- (34) Colabufo, N. A.; Berardi, F.; Contino, M.; Fazio, F.; Matarrese, M.; Moresco, R. M.; Niso, M.; Perrone, R.; Tortorella, V. Distribution of sigma receptor in EMT-6 cells: preliminary biological evaluation of PB167 and potential for in-vivo PET. *J. Pharm. Pharmacol.* **2005**, *57*, 1453–1459.

JM060639Z